ICNTC-2019 Special Issue

J. Indian Chem. Soc.,
Vol. 96, September 2019, pp. 1221-1226

An efficient method for the azocino[4,3-*b*]indole framework of strychnos alkaloids: DFT investigations on the electronic and spectroscopic properties

Nesimi Uludağ[a]*, Goncagül Serdaroğlu[b] and Naki Çolak[c]

[a]Department of Chemistry, Namık Kemal University, 59030, Tekirdag, Turkey

[b]Faculty of Education, Sivas Cumhuriyet University, 58140, Sivas, Turkey

[c]Department of Chemistry, Faculty of Sciences and Arts, Hitit University, 19030, Çorum, Turkey

E-mail: nuludag@nku.edu.tr, serdagroglu@cumhuriyet.edu.tr

Manuscript received online 26 April 2019, revised and accepted 20 July 2019

Tetracyclic 1,5-methanoazocino[4,3-*b*]indole (**2**) was achieved via a new synthetic approach for the synthesis of related strychnos alkaloids. These products embody the ABCD-ring system associated with the title alkaloids, as well as a one-pot construction of the ABCD ring system using tetrachloro-1,4-benzoquinone and tetrafluoro-1,4-benzoquinone, were involved as key steps. Also, the DFT-based quantum chemical calculations have been performed to evaluate the structural, electronic, and spectroscopic properties of the compound. PES (potential energy surface) scan revealed three stable conformers of the compound. The calculated FT-IR and NMR spectral data were compared with the corresponding observed values for the most stable conformer of the compound. Frontier Molecular Orbital analysis has revealed the chemical reactivity tendency and sites of the compound.

Keywords: Uleine, azocino[4,3-*b*]indole, FT-IR, NMR, NBO.

Introduction

The 1,5-methanoazocino[4,3-*b*]indole is one of the most-important biological subgroups of the strychnos alkaloids[1,2]. It is present in the unique structural features of their members and because of their critical pharmaceutical properties[3,4]. The 1,5-methanoazocino[4,3-*b*]indole tetracyclic ring system (ABCD rings) is believed to responsible for their antitumor[5] anti-HIV[6].

For these reasons, we report a new protocol for the cyclization of a 2-substituted tetrahydrocarbazoles bearing monosubstituted amide chains, leading to the desired 1,5-methanoazocino[4,3-*b*]indole via tetrachloro-1,4-benzoquinone and tetrafluoro-1,4-benzoquinone[7]. These reagents are used for the first time in the literature for the cyclization reaction (D-ring). Also, the quantum chemical calculations and analyses have been conducted to evaluate the structural and spectroscopic properties as well as the chemical reactivity tendency of the compound.

Experimental

12-Ethyl-2-methyl-6,6-ethylenedithio-1,2,3,4,5,6-hexahydro-1,5-methanoazocino[4,3-b]indole-3-one ***(2)***:The synthesis and measurement details of the compound were reported in the literature[7,18]. The residue was crystallized from diethyl ether to produce **2**. m.p. 206°C; IR (KBr): ν 3431 (N-H), 2958, 1637 (C=O) cm^{-1}; ^1H NMR (400 MHz, $CDCl_3$): δ 8.41 (s, 1H, N-H), 7.43 (d, 1H, *J* 7.7 Hz), 7.23 (d, 1H, *J* 8.3 Hz), 7.14 (t, 1H, *J* 8.1 Hz), 7.02 (t, 1H, *J* 7.3 Hz), 4.33 (d, 1H, *J* 1.6 Hz), 3.54–3.41 (m, 2H), 3.34–3.21 (m, 3H), 3.00 (s, 3H), 2.81–2.67 (m, 2H), 2.46 (t, 1H, *J* 7.5 Hz), 1.72–1.61 (m, 1H), 1.45–1.37 (m, 1H), 0.97 (t, 3H, *J* 7.2 Hz); ^{13}C NMR (100 MHz, $CDCl_3$): δ 169.3, 135.8, 132.3, 125.9, 122.8, 120.1, 118.2, 112.8, 111.1, 66.7, 52.9, 45.7, 44.1, 40.3, 39.5, 33.8, 34.1, 23.6, 11.7; Elemental Anal. Calcd. for $C_{19}H_{22}N_2OS_2$: C, 63.65; H, 6.19; N, 7.81. Found: C, 63.69; H, 6.22; N, 7.74.

Computational method:

All quantum chemical investigations of the compound

were performed by using the G09[8] package. First, the stable conformers of the compound were predicted by PES (potential energy surface) scan, at B3LYP/6-31G(d,p) level[9,10] in the gas phase. Then, three stable conformers were re-optimized at 6-311++G(d,p) level in both the gas phase and chloroform, and they were verified by having no imaginary frequency. PCM (polarized continuum model)[11] was used the chloroform phase calculations. PED (potential energy distribution) analysis was used to assign the vibrational frequencies by using the VEDA[12] package. Also, NMR shifts of the compound were calculated by GIAO (Gauge-Independent Atomic Orbital)[13,14] approaches to TMS. FMO (frontier molecular orbital)[15–17] investigation of the compound was performed to obtain the global reactivity tensors, i.e. the electronic chemical potential (χ), global hardness (η), electrophilicity (ω) and the maximum charge transfer index (ΔN_{max}), all equations are given as follow:

$$I = -E_{HOMO} \qquad A = -E_{LUMO}$$

$$\chi = \frac{I + t}{2} \qquad \eta = \frac{I + A}{2}$$

$$\omega = \frac{\mu^2}{2\eta} \qquad \Delta N_{max} = \frac{I + A}{2(I - A)}$$

Results and discussion

Our synthetic approach toward the tetracyclic core found in the uleine-type alkaloids was guided by a long-standing interest in developing a new approach of the intramolecular construction of the azocino[4,3-*b*]indole toward the synthesis of complex natural products. As illustrated in Scheme 1, our attention was focused on the closure of the D-ring. For this purpose, we selected a tetrahydrocabazole amide **(1)** as the starting material, which was synthesized previously described[18]. In this way, treatment of the amides with tetrachloro-1,4-benzoquinone in high yields (up to 98% yield) within 9 h under mild condition. Alternatively in this study, treatment of the 12-ethyl-2-methyl-6,6-ethylenedithio-1,2,3,4,5,6-hexahydro-1,5-methanoazocino[4,3-*b*]indole **(2)** in the presence of tetrafluoro-1,4-benzoquinone resulted in a cyclization reaction was obtained 63% yield (9 h). Further application of this method can be extended to the syntheses of the other members of the azocino[4,3-*b*]indole skeletal type alkaloids.

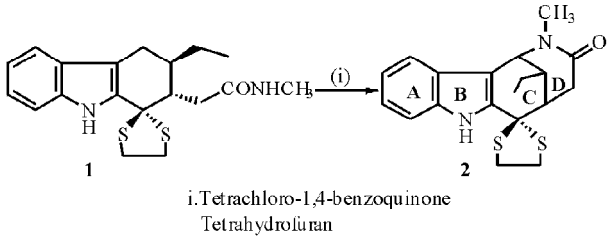

Scheme 1. Synthesis of the azocino[4,3-*b*]indole structure.

Molecular geometry and stability:

In this study, PES scan (Fig. 1) has been performed by B3LYP level according to the ethyl group orientation over the R**C** of the compound and revealed three stable structures. Fig. 1 and Fig. 2 show the dihedral angle used for the PES analysis and three stable structures on PES minima. Table 1 has summarized the selected geometric data and thermochemical quantities of all stable structures of the compound.

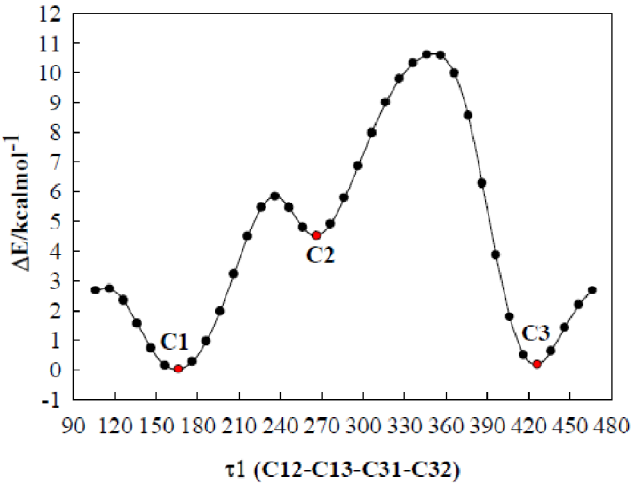

Fig. 1. The potential energy surface scan performed by the B3LYP/6-31G(d,p) level in the gas phase.

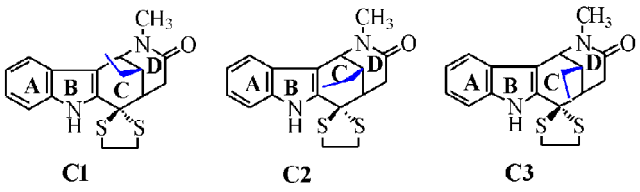

Fig. 2. The chemical structures of the lowest energy conformers of the compound.

Table 1. The selected geometric parameters in the chloroform phase and thermochemical quantities of three stable conformers of the title compound

	C1	**C2**	**C3**
Bond length (Å)			
N16-C4	1.38	1.38	1.38
N19-C24	1.36	1.36	1.36
O30-C24	1.23	1.23	1.23
S45-C38	1.88	1.88	1.88
S46-C38	1.90	1.90	1.90
Bond angle (°)			
C4-N16-C11	109.32	109.30	109.32
C14-N19-C24	121.49	121.12	121.51
N19-C24-O30	122.65	122.60	122.65
C20-C24-O30	118.99	118.94	119.01
S45-C38-S46	105.06	104.83	104.98
Dihedral angle (°)			
C4-N16-C11-C38	176.53	177.14	176.53
C14-N19-C24-O30	170.34	169.98	170.61
C14-N19-C24-C20	–13.12	–13.45	–12.82
N16-C11-C38-S45	–61.43	–61.88	–61.05
N19-C14-C13-C31	164.30	158.27	163.47
C14-C13-C31-C32	–70.77	34.97	–168.53
C12-C13-C31-C32	164.32	–93.92	66.35
ΔE_{total} (au)	–1718.327	–1718.319	–1718.327
ΔG (au)	–1718.378	–1718.369	–1718.377
$\Delta E_{rel.}$ (kcal/mol)	0.000	4.843	0.152
$\Delta G_{rel.}$ (kcal/mol)	0.000	5.208	0.312
μ (Debye)	6.546	6.457	6.507

From Table 1, the electronic energies (ΔE_{total}) for three conformers have been calculated as –1718.327, –1718.319 and –1718.327 au, respectively. Also, the relative free energies of these conformers are calculated between 0.000–5.208 kcal/mol. Here, the **C1** (conformer 1) is predicted as the lowest energy structure of the compound at –1718.327 au (electronic energy), whereas **C2** is estimated as the highest energy structure.

According to Table 1, the bond lengths and angles calculated for three structures are quite close to each other. For instance, the N16-C4, N19-C24, O30-C24 bond lengths for all structures are estimated at 1.38, 1.36, and 1.88 Å. Also, the C4-N16-C11, N19-C24-O30, S45-C38-S46 bond angles for **C1** are predicted at 109.32°, 122.65° and 105.06°, respectively. Also, C4-N16-C11-C38 angle for **C1**, **C2** and **C3** are determined as 176.53°, 177.14°, 176.53° respectively, with a deviation of approximately 3° from the planar. On the other hand, the scan angle (C12-C13-C31-C32) for **C1**, **C2,** and **C3** have been calculated as 164.32°, –93.92° and 66.35°, respectively. Similarly, the C14-C13-C31-C32 angle for three structures has been calculated as follows: –70.77° (**C1**), 34.97° (**C2**) and -168.53° (**C3**).

FT-IR spectral analysis:

Table 2 summarized the vibrational frequencies assigned by PED analysis and scaled by the factor 0.960[19] for the high-frequency region (>1700 cm^{-1}) and by 0.988 (<1700 cm^{-1}) for the remaining frequencies.

Table 2. The selected vibrational frequency (in cm^{-1}) assignments of the **C1** in the chloroform phase

Expt.	$S_{cal.}$	I_{IR}	PED (%)[a]
3431	3505	123	νNH (100)
	3063	28	νCH R**A** (94)
	3037	1	ν_{as}CH R**A** (93)
	3028	7	$\nu C_{26}H$ (89)
2938	2938	46	$\nu C_{39}H2$ (96)
	2904	53	$\nu C_{26}H3$ (96)
	2900	44	$\nu C_{32}H3$ (96)
	2892	28	$\nu C_{13}H$ (95)
1637	1643	730	ν(C=O) (80)
	1631	19	νCC R**AB** (57) + ipb HNC
	1592	1	νCC R**AB** (58) + ipb HNC
	1561	16	νCC R**ABC** (65)
	1503	20	$\sigma C_{26}H2$ (32) + $\nu N_{19}C$ (22)
	1502	22	νCC R**A** (21) + ipb (HNC + HCC R**A)** (38)
	1460	2	$\sigma(C_{39}H2 + C_{40}H2)$ (88)
	1450	43	ipb HNC (21)
	1410	68	$sbC_{26}H3$ (54) + $\sigma C_{26}H2$ (14)
	1393	6	$sbC_{32}H3$ (78)
	1369	7	$\nu(N_{16}C + CC$ R**A**) (15)
	1302	12	$\nu(N_{16}C + N_{19}C)$ (22)
	1233	37	$\nu N_{19}C$ (31) + $\omega C_{31}H2$ (32)
	1218	48	ipb HNC (50)
	1168	36	νCC R**AC** (24) + ipb HNC
	1155	4	ipb HCC R**A** (59)
	1128	19	$\omega C_{26}H2$ (57)+ $\sigma C_{26}H2$ (15)
	1123	2	ipb HCC R**A** (38) + νCC R**A** (19)
	1005	22	$\nu N_{19}C$ + νCC R**ABC** (19)
	969	0	opb HCC R**A** (83)
	962	26	ρ CH2 R**E** (54)
	935	11	$\nu N_{19}C$ + νCC (37)

Table-2 (contd.)

892	3	α R**A** + ipb HNC (60)
831	6	$\nu N_{19}C$ + νCC R**ABC** (11)
782	25	νCS (10) + opb CSC (26)
753	19	$\nu N_{19}C$ (10) + χHCCN (11)
742	101	opb HCC R**A** (86)
699	20	opb (HCC R**A** + HNC) (10)
677	1	νCS (75)
663	6	νCS (88)
639	16	ν(CC R**A** + NC) (30)
443	6	opb HCC R**A** (49) + νNC (10)
414	31	opb HNC (15)
408	46	opb HNC (86)

*The abbreviations are as I_{IR}, IR intensity; ν, symmetric stretching; ν_{as}, asymmetric stretching; ω, wagging; τ, twisting; ρ, rocking; σ, scissoring; α, in-plan ring deformation; β, non-planar ring deformation; ipb, in-plane bending; opb, out-plane bending; sb, symmetric bending; χ, torsion; R, ring.

It was reported that the N-H stretching band related to the primary and secondary amines for the heterocyclic aromatic compounds appeared in the range of 3000–3500 cm^{-1} [20,21]. In this work, we have observed the N-H stretching band at 3431 cm^{-1} and assigned by PED analysis at 3505 cm^{-1} (100%). Also, the ipb HNC and opb HNC bending modes have been calculated in the range of 1631–892 cm^{-1} and 699–408 cm^{-1} with variable IR intensity, respectively. Also, the N-C band for the imidazoline and benzimidazole derivatives was observed in 1600 and 1510 cm^{-1} [22] and assigned by PED in the range of 1680–1386 cm^{-1} for the hydrazine derivatives[23]. In this study, we have assigned νNC mode in the field of 1503–443 cm^{-1}; but it should be noticed that the signal attributed in 1302 cm^{-1} is predicted as a pure N-C mode whereas the other νNC signals are assigned as the mixed with the other vibrational modes.

Recently, it was reported that the carbonyl group stretching (νC=O) signal for the substituted carbazole compounds appeared in the range of 1643–1633 cm^{-1} [24]. As expected, the very strong peak occurred at 1637 cm^{-1} has been assigned by PED at 1643 cm^{-1} (80%) as a pure νC=O stretching mode.

In the literature, the phenyl ring C-H stretching mode was observed in 3086–3026 cm^{-1} and calculated by B3LYP level in 3212–3133 cm^{-1} [25]. Here, the aromatic and aliphatic C-H stretching frequencies of the compound have been assigned by PED in the range of 3063–3037 cm^{-1} and 3028–2892 cm^{-1}, respectively. From Table 2, the symmetric stretching modes ($sbCH_3$) for the methyl groups have been assigned at 2904 (96%) and 2900 cm^{-1} (96%). Also, the ipb HCC and opb HCC bending modes for the aromatic ring have been calculated in the range of 1502–1123 cm^{-1} and 969–443 cm^{-1}, respectively. As expected, the aromatic C-C stretching modes of the compound have been estimated in the field of 1631–639 cm^{-1} with variable intensity, and generally as a mixed mode. Namely, the assigned νCC signals at 1631, 1592, 1502, 1369, and 1168 cm^{-1} have been contaminated with the ipb HNC mode. On the other hand, the predicted signal at 1561 cm^{-1} (65%) is related to the aromatic νCC stretching mode coupled with the aliphatic νCC stretching modes of the compound.

NMR spectral analysis:

The recorded and calculated NMR isotropic shifts of the most stable conformer of the compound have been given in Table 3.

As known well, the carbon atoms for the aromatic sys-

Table 3. The observed and calculated NMR chemical shifts (in ppm) of the compound in the chloroform phase

	^{13}C NMR			^{1}H NMR	
	Expt.	Calcd.		Expt.	Calcd.
C1	120.1	126.3	H7	7.02	7.4
C2	122.8	129.8	H8	7.14	7.5
C3	111.1	116.5	H9	7.23	7.5
C4	135.8	144.2	H10	7.43	7.9
C5	125.9	134.6	H17	8.41	8.1
C6	118.2	124.8	H18	4.33	4.5
C11	132.3	140.8	H21	3.00	2.7
C12	45.7	57.6	H22	2.74	2.5
C13	44.1	53.0	H23	3.00	3.4
C14	52.9	57.3	H25	2.74	2.5
C15	112.8	122.9	H27	2.46	2.5
C20	33.8	44.7	H28	3.48	4.1
C24	169.3	177.4	H29	3.00	2.6
C26	34.1	35.6	H33	1.67	1.8
C31	23.6	31.5	H34	1.41	1.4
C32	11.7	15.7	H35	0.97	1.2
C38	66.7	88.6	H36	0.97	0.9
C39	40.3	51.9	H37	0.97	1.2
C40	39.5	50.1	H41	3.48	3.7
			H42	3.28	3.5
			H43	3.28	3.4
			H44	3.28	3.4

tems gave a peak in the range of ~110–180 ppm in the NMR spectra depend on the chemical environment[26–28]. Recently, Sekar and coworkers[29] reported the carbon shifts for the carbazole-chromophores in the range of 156.62–197.68 ppm, they observed the highest chemical shift was recorded for the 3-acetyl-9-hexyl-carbazole compound because of the oxygen atom. Here, we have observed the ^{13}C NMR chemical shifts (C1-C6) for the phenyl ring in 111.1–135.8 ppm and have calculated in 116.5–144.2 ppm. As expected, the highest chemical shift has been recorded in 169.3 ppm and computed in 177.4 ppm for the C24 atom, which bonded to an oxygen atom and neighboring to the nitrogen atom. Besides, the ^{1}H NMR shifts for the aromatic hydrogen atoms (H7-H10) have been observed in the range of 7.02–7.43 ppm and assigned by B3LYP level in 7.4–7.9 ppm. Also, it can be seen from Table 3 that the proton shifts for the methyl group (H35, H36, H37) gives a triplet peak at 0.97 ppm in the spectrum, whereas it is calculated by B3LYP in the range of 0.9–1.2 ppm. Besides, the ^{1}H shift for the proton bonded to the nitrogen atom of the indole part of the compound is calculated in 8.1 ppm and observed in 8.41 ppm. In the literature, the proton chemical shifts for the unsaturated rings were observed in 8.15–9.07 ppm[26] and calculated by the B3LYP/6-311++G(d,p) level in 7.85–811 ppm[30].

Also, we have looked for the relationship between the observed and calculated NMR chemical shifts, and the correlation equations have been given below:

$$\delta_{exp\text{-}C} = 0.9961\delta_{calc\text{-}C} + 8.8720 \ (R^2 = 0.9923, S = 4.34)$$

$$\delta_{exp\text{-}H} = 0.9622\delta_{calc\text{-}H} + 0.0344 \ (R^2 = 0.9869, S = 0.26)$$

Accordingly, the regression coefficients for the ^{13}C and ^{1}H NMR isotropic shifts have been calculated as R^2 = 0.9923 and R^2 = 0.9869 respectively which indicated the observed and recorded NMR shifts are in a good agreement with each other.

Chemical reactivity descriptors, FMO analysis, MEP diagrams:

For a long time, frontier molecular orbitals and related quantum chemical tensors have been used to predict the chemical reactivity and stability tendency of the molecular systems[31,32]. In this work, we have performed the FMO analyses to obtain the global reactivity parameters for the stable conformers of the compound to interpret the reactivity behavior of the compound. All calculated parameters have been given in Table 4, in both the vacuum and chloroform.

Table 4. The quantum chemical reactivity identifiers for the compound in chloroform

	Chloroform		
	C1	**C2**	**C3**
HOMO (-I)	–0.2162	–0.2158	–0.2161
LUMO (-A)	–0.0414	–0.0414	-0.0414
ΔE_{gap}	4.7555	4.7443	4.7549
χ	–3.5048	–3.4998	–3.5037
η	2.3777	2.3722	2.3775
ω	2.5831	2.5817	2.5818

*ΔE_{gap}, χ, η, ω and ΔN_{max} are in eV; HOMO and LUMO energies are in au.

From Table 4, the reactivity descriptors in chloroform have been changed in the following order:

ΔE_{gap} (Energy gap) : **C1 > C3 > C2**

χ (Electronic chemical potential) : **C2 > C3 > C1**

η (Global hardness) : **C1 > C3 > C2**

ω (Electrophilicity index) : **C2 > C3 > C1**

ΔN_{max} (Charge transfer capability) : **C2 > C3 > C1**

Accordingly, the **C1** has the highest kinetic stability while the **C2** has the lowest stability, because of the ΔE_{gap} values of them. Also, the **C1** is both the hardest conformer and the less electrophile as well as having the lowest charge transfer capability because of the ordering of the η, ω, and ΔN_{max} parameters.

Fig. 3 shows the HOMO, LUMO and MEP pilots of three

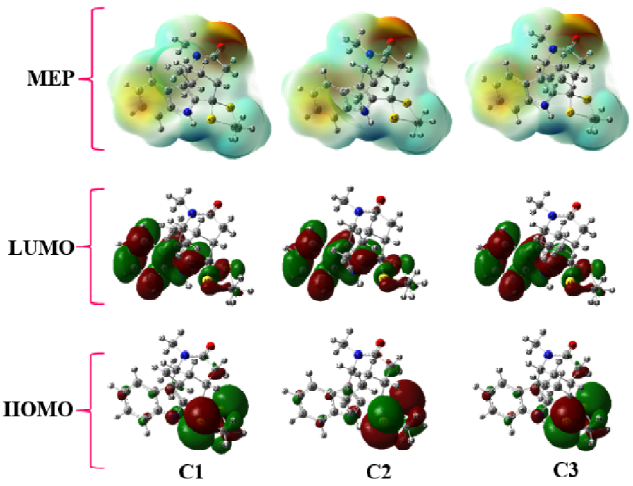

Fig. 3. HOMO, LUMO (isoval:0.02) and MEP (isoval:0.0004) plots for the conformers of the title compound at B3LYP in the chloroform phase.

stable conformers of the compound. For all conformers, the HOMO as a nucleophilic attack center is localized on the R**E**, whereas LUMO as an indicator of electrophilic attack site is localized on the R**A**, R**B**, and R**E**. Moreover, the electron-rich region (red) of all conformers is determined around of the oxygen (O30) atom and partly on the R**A**, whereas the electron-poor area (blue) of the conformers is estimated mostly around of the nitrogen (N16) atom and partly on the remaining part of the conformers.

Conclusions

The work reported here, when considered in conjunction with our previous studies, serves to emphasize the essential utility of both tetrachloro-1,4-benzoquinone and tetrafluoro-1,4-benzoquinone when these are applied together within a given synthetic sequence. Such processes in the assembly of other relevant heterocyclic frameworks of azocino[4,3-*b*]indole are going on studies in our laboratories. It should also be noted that rather efficient methods for the synthesis of the azocino[4,3-*b*] in one step using amide **1,** as a starting material. Critical to the success of our synthetic plan was the efficient construction of the cyclization D-ring. To this end, we have completed an efficient synthesis of the azocino[4,3-*b*]indole skeleton. The observed spectroscopic data are a good agreement with the corresponding calculated data. Also, this work shows that the HOMO as a nucleophilic attack center is localized on the R**E**, whereas LUMO as an indicator of electrophilic attack site is localized on the R**A**, R**B**, and R**E**.

Acknowledgements

This work was supported by Sivas Cumhuriyet University, Scientific Research Projects Department (Grant No. CUBAP: EĞT-072). All calculations have been carried out at TUBITAK ULAKBIM, High Performance and Grid Computing Center (TR-Grid e-Infrastructure).

References

1. J. Schmutz, F. Hunziker and R. Hirt, *Helv. Chim. Acta*, 1957, **40**, 1189.
2. J. A. Joule, M. Ohash, B. Gilbert and C. Djerassi, *Tetrahedron,* 1965, **21**, 1717.
3. Z. E. Dos Santos Torrees, E. R. Siiveria, L. F. Roche e Silva, E. S. Lima, M. De Vasconcellos, D. De Andrade Uchoa, R. B. Filho and A. M. Pohlit, *Molecules,* 2013, **18**, 62681.
4. T. P. Chierrito, A. C. C. Aguiar, I. M. De Andrade, I. P. Ceravolo, R. A. C. Gonçalves, A. J. B. Oliveria and A. U. Krettli, *Malara J.,* 2015, **13**, 142.
5. J. Bonjoch and D. Sole, *Chem. Rev.,* 2000, **100**, 3455.
6. T. Ohsima, Y. Xu, R. Taxita, S. Shimizue, D. Zhong and M. Shibasaki, *J. Am. Chem. Soc.,* 2002, **124**, 14546.
7. (a) N. Uludag and M. Yakup, *Org. Prep. Proc. Int.,* 2015, **47**, 454; (b) N. Uludag, *Org. Prep. Proc. Int.,* 2019, **51**, 294.
8. Gaussian 09, Revision D.01, Gaussian, Inc, Wallingford CT, 2013.
9. A. D. Becke, *J. Chem. Phys*., 1993, **98**, 1372.
10. C. Lee, W. Yang and R. G. Parr, *Phys. Rev. B*, 1988, **37**, 785.
11. J. Tomasi, B. Mennuci and R. Cammi, *Chem. Rev*., 2005, **105**, 2999.
12. M. H. Jamroz, Vibrational Energy Distribution Analysis VEDA 4, Warsaw, 2004-2010.
13. C. M. Rohlfing, L. C. Allen and R. Ditchfield, *Chem. Phys*., 1984, **87**, 9.
14. K. Wolinski, J. F. Hinton and P. Pulay, *J. Am. Chem. Soc.,* 1990, **112**, 8251.
15. T. Koopmans, *Physica*, 1934, **1**, 104.
16. R. G. Parr, L. V. Szentpaly and S. Liu, *J. Am. Chem. Soc.,* 1999, **121**, 1922.
17. R. G. Parr and R. G. Pearson, *J. Am. Chem. Soc.,*1983, **105**, 7512.
18. S. Patir and N. Uludag, *Tetrahedron,* 2009, **65**, 115.
19. A. Borba, M. Albrecht, A. Gomez-Zavaglia, L. Lapinski, M. J. Nowak, M. A. Suhm and R. Fausto, *Phys. Chem. Chem. Phys*., 2008, **10**, 7010.
20. G. Serdaroglu and N. Uludag, *Bulg. Chem. Commun*., 2018, **50**, 25.
21. M. Mohseni, S. Akbari, E. Pajootan and F. Mazaheri, *Environ. Sci. Pollut. Res.,* 2019, **26**, 12689.
22. E. Üstün, S. D. Düşünceli and I. Özdemir**,** *Struct. Chem*., 2019, **30**, 769.
23. K. Sayın, *Spectrochim. Acta **A***, 2019, **212**, 380.
24. M. L. Kadam, D. Patil and N. Sekar, *Opt. Mater*., 2018, **85**, 308.
25. G. Vengatesh and M. Sundaravadivelu, *Res. Chem. Intermediat.,* doi.org/10.1007/s11164-019-03838-9.
26. M. Fizer, O. Fizer, V. Sidey, R. Mariychuk and Y. Studenyak, *J. Mol. Struct*., 2019, **1187**, 77.
27. J. Liu, Z. Zhang, L. Yang, Yongming Fan and Y. Liu, *J. Mol. Grap. Model*., 2019, **88**, 228.
28. B. Tüzün and K. Sayýn, *Spectrochim. Acta A*, 2019, **208**, 48.
29. P. K. M. Lokhande, D. S. Patil and N.Sekar, *J. Lumin*., 2019, **211**, 162.
30. G. Serdaroğlu and N. Şahin, *J. Mol. Struct*., 2019, **1178**, 212.
31. R. A. Y. Kamsi, G. W. Ejuh, Y. T. Assatse, C. A. Njeumen, F. Tchoffo and J. M. B. Ndjaka, *Chinese J. of Phys*., 2019, **60**, 1.
32. J. Aihara. *J. Phys. Chem. A*, 1999, **103**, 7487.